

Journal of Applied Fluid Mechanics, Vol. 11, No. 5, pp. 1321-1331, 2018.
Available online at www.jafmonline.net, ISSN 1735-3572, EISSN 1735-3645.
DOI: 10.29252/jafm.11.05.28745

A Study on the Effect of Peristalsis and Cilia of MHD Micropolar Fluid Flow through an Inclined Porous Channel

S. V. H. N. Krishna Kumari. P^{1†}, D. Saroj Vernekar² and Y. V. K. Ravi Kumar³

¹ Department of Mathematics, Koneru Lakshmaiah Educational Foundation, Hyderabad, India

² Department of Mathematics, Stanley College of Engineering and Technology for Women, Hyderabad.

³ Birla Institute of Technology & Science (BITS)-Pilani, Hyderabad, India.

[†] Corresponding Author Email: krishnagannamaraju@gmail.com

(Received December 31, 2017; accepted March 13, 2018)

ABSTRACT

The study of the influence of magnetic field, channel inclination, porous medium and cilia on the Micropolar fluid under different boundary conditions is carried out. The methods of solving Navier Stokes equation specific to Micropolar fluid under the joint influence of these effects are presented. The profiles of velocity (along the flow direction), the micro rotation vector and the variation of pressure rise with time average flow rate for fixed values of other parameters were carried out and the results are discussed.

Keywords: Micropolar fluid, Peristalsis, Cilia, Magnetic field, Porous medium.

NOMENCLATURE

τ_{ij}	Cauchy stress tensor,	λ	wavelength
S_{ij}	Micro stress average,	$\frac{c}{\bar{X}_0}$	wave speed of the metachronal wave
\mathcal{E}_{ijk}	First stress moments,	I	reference position of the particle unit tensor,
V	velocity vector	ϵ_{kij}	alternating tensor
V	component in the axial direction),	\dot{S}_k	micro inertial rotation
F_j	body force per unit mass,	$\alpha_v, \beta_v, \gamma$	spin gradient viscosity coefficients.
\dot{S}_{jk}	spin inertia	σ_e	electrical conductivity of the fluid,
L_{jk}	body couple.	B_0	magnetic flux,
(,)	comma after a suffix denotes covariant differentiation,	θ	angle of inclination,
	$\{\Omega_i\}$ micro rotation vector	k_0	permeability parameter
C_{ik}	couple stress tensor	g	acceleration due to gravity.
λ_v	dilation(bulk) viscosity coefficient,	b	amplitude,
μ	classical shear viscosity coefficient	Da	Darcy's number
k	vortex viscosity coefficient unit tensor,	α_1	slip parameter
p	isotropic pressure,	β	Dimensionless wave number,
d	rate of deformation tensor	Λ	wavelength the metachronal wave.
a	mean breadth of the ciliated channel,	q	volume flux
ϵ	non-dimensional measure w.r.t cilia length,	u	fluid velocity
α	measure of the eccentricity of the elliptical motion of the particle.	Δp	pressure rise
		m	Micropolar parameter,
		M	magnetic parameter,
		N	Coupling number

1. INTRODUCTION

It is well known that mixing and transporting of physiological fluids is referred as peristalsis, which is generated due to progressive waves of area contraction and expansion along the length of a distensible tube containing fluid. Peristalsis occurs widely in the functioning of the ureter, food mixing and chyme movement in the intestine, movement of eggs in the fallopian tube, the transport of the spermatozoa in cervical canal, transport of bile in the bile duct, transport of cilia, and circulation of blood in small blood vessels. The peristaltic transports through tubes/channels have attracted considerable attention due to their wide applications in medical and engineering sciences. Motivated by these facts, a good number of analytical, numerical and experimental studies have been conducted to understand peristaltic action under different conditions with reference to physiological and mechanical situations.

Magneto hydrodynamics is the dynamics of magnetic fields in electrically conducting fluids. Many researchers have considered MHD flows of viscous electrically conducting fluids inside channels for various situations. [Gribben \(1965\)](#) discussed the Magneto hydrodynamic boundary layer in the presence of a pressure gradient. [Moreu \(1990\)](#) in his book Magneto hydrodynamics gave the conclusions on the system of equations of MHD.

A porous medium is a multi phase material and is characterized by its porosity, permeability, tensile strength and electrical conductivity. These properties are derived from the respective properties of its constituents (solid matrix and fluid). The flow in a porous medium can be described using either by Darcy's law or non-Darcy's law. Research was done on dynamics of fluids in porous media by [Bear J \(1972\)](#) which helped in developing of joint probability distributions of soil water retention characteristics.

[El.Shehawy \(1999,2000\)](#) investigated peristaltic transport through a porous medium and effects of porous boundaries on peristaltic transport through a porous medium. [Mekheimer \(2003\)](#) studied the linear peristaltic transport through a porous medium in an inclined planar channel. Peristaltic pumping of a Jeffrey fluid with variable viscosity through a porous medium in a planar channel was discussed by [Subba Reddy \(2010\)](#). [Krishna Kumari *et al* \(2011\)](#) discussed peristaltic pumping of a Jeffrey fluid and MHD Casson Fluid in an inclined channel

Cilia are little appendages that stick out from eukaryotic cells. They whip back and forth and help cells move around in cellular fluids. They also help particles move past the cell. They generally occur one per cell, examples of primary cilia can be found in human sensory organs such as the eye and the nose. Another important feature of ciliated cells is the existence of waves propagating all along the surface. These are called metachronal waves and might be due to the coordination of

adjacent cilia, for example, via hydrodynamic interactions. [Boris Guirao and Jean-Francois Joanny \(2017\)](#) observed experimentally that metachronal waves propagate in all possible directions, in the direction of the effective stroke (symplectic metachronal waves), in the opposite direction (antiplectic), or even in a perpendicular direction (laeoplectic or dexioplectic) or oblique direction. Metachronal waves are produced when a group of cilia operate together, and it applies a force on the fluid to move it in the direction of the effective stroke. In the last few years considerable success in the modeling of cilia and the understanding of their fluid mechanical interaction to explain either propulsion or fluid transport has been observed. [Siddiqui \(2015\)](#) developed a mathematical model for the flow of a Casson fluid due to metachronal beating of cilia in a tube. Recently [Nadeem \(2017\)](#) analyzed metachronal wave for non-Newtonian fluid inside a symmetrical channel with ciliated walls and the physical hydrodynamic propulsion model on creeping viscous flow through a ciliated porous tube was studied by [Akbar \(2017\)](#).

Research in molecular biology, microcirculation, and micro fluidics reveal that fluids like blood, polymeric suspensions etc. have individual particles of different sizes around a micron with complex structures that can rotate or change shape thus altering the macroscopic properties which was identified by [Eringen \(1965\)](#). Micropolar fluids are treated as a special case of micro continuum fluids, in which, only the rotational aspect of the particle is considered. Physically, Micropolar models represent fluids whose molecules can rotate independently of the fluid stream and its local vorticity. The occurrence of the Microrotation vector, which differs from the stream flow vorticity vector and from the angular velocity, results in the formation of non-symmetric stresses and coupled stresses, which consequently result in an increase in the energy dissipation.

[Arimon and Cakmak \(1968\)](#) discussed three basic viscous flows of Micropolar fluids. [Devanathan \(1975\)](#) investigated peristaltic motion of a Micropolar fluid. [Srinivasacharya \(2003\)](#) studied peristaltic pumping of a Micropolar fluid in a tube. [Muthu *et al* \(2003\)](#) discussed peristaltic motion of Micropolar fluid in circular cylindrical tubes, [Hayat \(2008\)](#) studied peristaltic flow of a Micropolar fluid in an asymmetric channel. [Satyanarayana \(2016\)](#) studied MHD peristaltic transport of a Micropolar fluid in an asymmetric channel with porous medium. However, literature survey indicates that no attention was given to analyze ciliated effect on Micropolar fluid in the presence of porous medium and magnetic field. The study was then extended to find the effect of peristalsis and cilia on the flow rate of Micropolar fluid under identical conditions and a comparative study on the properties is carried out.

2. MATHEMATICAL FORMULATION

Under the assumption that the channel length is an integral multiple of the wavelength λ and the

pressure difference across the ends of the channel is a constant, the flow becomes steady in the wave frame (\bar{x}, \bar{y}) moving with velocity c away from the fixed (laboratory) frame (\bar{X}, \bar{Y}) . The transformation between these two frames is given by

$$\bar{x} = \bar{X} - c\bar{t}; \bar{y} = \bar{Y}; \bar{u}(x, y) = \bar{U}(\bar{X} - c\bar{t}, \bar{Y}); \bar{v}(x, y) = \bar{V}(\bar{X} - c\bar{t}, \bar{Y})$$

The equation of conservation of mass is

$$\frac{\partial \rho}{\partial t} + (\rho V_i)_{,i} = 0 \tag{1}$$

Balance of linear momentum

$$\tau_{ij,i} + \rho \left(F_j - \dot{v}_j \right) = 0 \tag{2}$$

Balance of first stress moments

$$\tau_{ij} - s_{ij} \mathcal{E}_{ijk,k} + \rho \left(L_{jk} - \dot{S}_{jk} \right) = 0 \tag{3}$$

where $v_{i,j} = \frac{\partial v_i}{\partial x_j}$, $\dot{v}_i = \frac{\partial v_i}{\partial t} + v_{i,j} v_j$. The

results of linear constitutive theory of Micro-isotropic fluids as outlined by Eringen (1965) are

$$\tau = (-p + \varepsilon \text{tr}(d) + \lambda_0 \text{tr}(b-d))I + 2\mu_1 d + 2\mu_2(b-d) + 2\mu_3(b^T - d) \tag{4}$$

$$S = (-p + \varepsilon \text{tr}(d) + \eta_0 \text{tr}(b-d))I + 2\mu_1 d + \zeta_1(b - b^T - 2d) \tag{5}$$

$$\begin{aligned} \mathcal{E}_{ijk} = & (\gamma_1 a_{kr} + \gamma_2 a_{rkr} + \gamma_3 a_{rrk}) \delta_{ij} + \\ & (\gamma_4 a_{jrr} + \gamma_5 a_{rjr} + \gamma_6 a_{rrj}) \delta_{ik} + \\ & (\gamma_7 a_{irr} + \gamma_8 a_{rir} + \gamma_9 a_{rri}) \delta_{jk} + \\ & \gamma_{10} a_{ijk} + \gamma_{11} a_{ikj} + \gamma_{12} a_{jik} + \\ & \gamma_{13} a_{kij} + \gamma_{14} a_{jki} + \gamma_{15} a_{kji} \end{aligned} \tag{6}$$

with,

$$\begin{aligned} d_{ij} = & \frac{1}{2}(v_{i,j} + v_{j,i}), b_{ij} = v_{i,j} - v_{j,i}, \\ a_{ijk} = & \Omega_{ijk} \end{aligned} \tag{7}$$

A micro fluid will be called Micropolar if for all motions

$$\begin{aligned} \mathcal{E}_{ijk} = & -\mathcal{E}_{ikj}, \\ \Omega_{ij} = & -\Omega_{ji} \Rightarrow a_{ijk} = -a_{jik} \end{aligned} \tag{8}$$

Micropolar fluids exhibit only micro-rotational effects and can support surface and body couples. Fluid points contained in a small volume element, in addition to its usual rigid motion, can rotate about the centric of the volume element in an

average sense described by the gyration tensor Ω .

Equation (6) is valid for all motions if

$$\begin{aligned} \gamma_1 - \gamma_2 + \gamma_4 - \gamma_5 = & 0, \\ \gamma_7 - \gamma_8 = & 0, \gamma_{10} - \gamma_{12} + \gamma_{11} - \gamma_{13} = & 0 \end{aligned} \tag{9}$$

Using Eq. (9) in Eq. (6), we get

$$\begin{aligned} \mathcal{E}_{ijk} = & (\gamma_1 - \gamma_2)(a_{kkk} \delta_{ij} - a_{jkk} \delta_{ik}) + \\ & (\gamma_{10} - \gamma_{12})(a_{ijk} - a_{ikj}) + (\gamma_{14} - \gamma_{15}) a_{jki} \end{aligned} \tag{10}$$

In view of skew-symmetry conditions (8) the independent number Ω_{ij} and \mathcal{E}_{ijk} are respectively 3 and 9.

Introducing two new sets of variables we get ω_k and C_{ij} by

$$\omega_k = \frac{1}{2} \epsilon_{kij} \Omega_{ij}, C_{ik} = -\epsilon_{kji} \mathcal{E}_{ijk}, \tag{11}$$

Similarly we introduce

$$\begin{aligned} \dot{S}_k = & -\epsilon_{kij} \dot{S}_{ij}, \dot{S}_{ij} = -\gamma \epsilon_{kij} \dot{S}_k, \\ L_k = & -\epsilon_{kij} L_{ij}, L_{ij} = -\gamma \epsilon_{kij} L_k \end{aligned} \tag{12}$$

The constitutive Eq. (6) can be put in the form

$$\tau_{ij} = (-p + \lambda_v v_{k,k}) \delta_{ij} + \mu(v_{i,j} + v_{j,i}) + k(v_{j,i} - \epsilon_{ijk} \Omega_k) \tag{13}$$

with $\mu_0 - \mu_1 + \mu_2 = \mu$, $2(\mu_2 - \mu_1) = k$

Rewriting Eq. (13) we get

$$\tau_{ij} = (-p + \lambda_v D_{kk}) \delta_{ij} + (2\mu + k) D_{ij} - k \epsilon_{ijk} (\omega_k + \Omega_k) \tag{14}$$

with $\omega_{ij} = -\epsilon_{ijk} \omega_k = \frac{1}{2}(v_{i,j} - v_{j,i})$

Multiplying Eq. (10) with ϵ_{ijk} and using Eqs. (11) and (12), we get

$$C_{ij} = \alpha_v \Omega_{k,k} \delta_{ij} + \beta_v \Omega_{i,j} + \gamma \Omega_{j,i} \tag{15}$$

$$\begin{aligned} \alpha_v = & 2(\gamma_{12} - \gamma_{15}), \beta_v = 2(\gamma_2 - \gamma_1), \\ \gamma = & 2(\gamma_1 - \gamma_2 + \gamma_{10} - \gamma_{12} - \gamma_{14} + \gamma_{15}) \end{aligned}$$

Now the field equations satisfied by ρ , v_i and Ω_i are given by

$$\frac{\partial \rho}{\partial t} + (\rho V_i)_{,i} = 0$$

$$-p_{,i} + (\lambda_v + \mu)v_{j,i,j} + (\mu + k)v_{i,j,j} + k \in_{ijk} \Omega_{k,j} + \rho(F_i - \dot{v}_i) = 0 \quad (16)$$

$$(\alpha_v + \beta_v)v_{j,i,j} + \gamma v_{i,j,j} + k \in_{ijk} v_{k,j} - 2k\Omega_i + \rho(L_i - j\dot{\Omega}_i) = 0 \quad (17)$$

$$-p_{,i} + (\lambda_v + \mu)v_{j,i,j} + (\mu + k)v_{i,j,j} + k \in_{ijk} \Omega_{k,j} + \rho(F_i - \dot{v}_i) = 0$$

$$(\alpha_v + \beta_v)v_{j,i,j} + \gamma v_{i,j,j} + k \in_{ijk} v_{k,j} - 2k\Omega_i + \rho(L_i - j\dot{\Omega}_i) = 0 \quad (18)$$

j is the fluid micro gyration parameter and the dot notation is used for the material derivatives given by $\dot{v}_i = \frac{\partial v_i}{\partial t} + v_{i,j}v_{j,i}$, $\dot{\Omega}_i = \frac{\partial \Omega_i}{\partial t} + \Omega_{i,j}\Omega_j$ (19)

The equation of continuity is

$$\frac{\partial \bar{u}}{\partial x} + \frac{\partial \bar{v}}{\partial y} = 0 \quad (20)$$

Introducing the Micropolar principles into Navier Stokes formulation in the presence of magnetic field, porous medium and inclination results the following equations.

$$\rho \left[\bar{u} \frac{\partial \bar{u}}{\partial x} + \bar{v} \frac{\partial \bar{u}}{\partial y} \right] = - \frac{\partial \bar{p}}{\partial x} + (\mu + k) \left[\frac{\partial^2 \bar{u}}{\partial x^2} + \frac{\partial^2 \bar{u}}{\partial y^2} \right] + k \frac{\partial \bar{\Omega}}{\partial y} - \left(\sigma_e B_0^2 + \frac{\mu}{k_0} \right) (\bar{u} + c) + g \sin \theta \quad (21)$$

$$\rho \left[\bar{u} \frac{\partial \bar{v}}{\partial x} + \bar{v} \frac{\partial \bar{v}}{\partial y} \right] = - \frac{\partial \bar{p}}{\partial y} + (\mu + k) \left[\frac{\partial^2 \bar{v}}{\partial x^2} + \frac{\partial^2 \bar{v}}{\partial y^2} \right] + k \frac{\partial \bar{\Omega}}{\partial x} - \left(\sigma_e B_0^2 + \frac{\mu}{k_0} \right) \bar{v} \quad (22)$$

$$\rho \left[\bar{u} \frac{\partial \bar{\Omega}}{\partial x} + \bar{v} \frac{\partial \bar{\Omega}}{\partial y} \right] = \gamma \frac{\partial^2 \bar{\Omega}}{\partial y^2} - k \left(2\bar{\Omega} + \frac{\partial \bar{u}}{\partial y} \right) \quad (23)$$

It is assumed that the plates are very wide and long so that the flow is essentially axial ($u \neq 0, v = 0$). Further, the flow is considered far downstream from the entrance so that it can be treated as fully-developed.

From the continuity equation we get

$$\frac{\partial \bar{u}}{\partial x} = 0 \Rightarrow \bar{u} = \bar{u}(y) \quad (24)$$

As it is obvious from Eq. (23), that there is only a single

non-zero velocity component that varies across the channel. So, only x-component of Navier-Stokes equation can be considered for this planner flow.

Introducing the non-dimensional variables, we get

$$x = \frac{\bar{x}}{\lambda}, y = \frac{\bar{y}}{a}, u = \frac{\bar{u}}{c}, v = \frac{\lambda \bar{v}}{ac}, \Omega = \frac{\bar{\Omega}}{c}, p = \frac{a^2 \bar{p}}{c\lambda}, t = \frac{c\bar{t}}{\lambda}$$

$$M^2 = \frac{\sigma_e B_0^2 a^2}{\mu c}, G = \frac{g a^2}{\mu c^2} \quad (25)$$

The non-dimensional governing equations of the fluid flow are

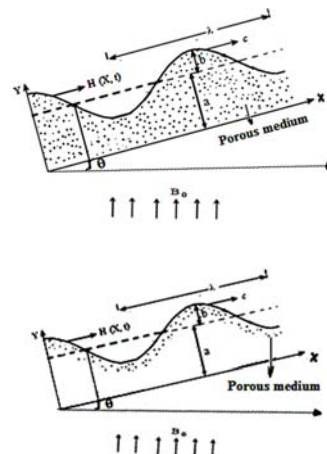
$$\frac{\partial^2 u}{\partial y^2} + N \frac{\partial \Omega}{\partial y} - (1-N)(M^2 + \sigma^2)(u+1) = (1-N) \left[\frac{\partial p}{\partial x} - G \sin \theta \right] \quad (26)$$

$$\left(\frac{2-N}{m^2} \right) \frac{\partial^2 \Omega}{\partial y^2} - \frac{\partial u}{\partial y} - 2\Omega = 0 \quad (27)$$

where $N = \frac{k}{(\mu + k)}$ is coupling number ($0 \leq N \leq 1$), $m = \sqrt{j^2 k (2\mu + k) / \gamma (\mu + k)}$ is the Micro-polar parameter. N and m are the two parameters which characterize the Micropolar fluid and makes it different from the Newtonian fluid in the limiting case of $N \rightarrow 0, m \rightarrow 0$.

2.1 Flow With Peristaltic Pumping

Consider the peristaltic pumping of a Micropolar fluid in an inclined channel of half-width 'a'. A longitudinal train of progressive sinusoidal waves take place on the upper and lower walls of the channel. For simplicity we restrict our discussion to the half-width of the channel as shown in Fig. 1.



Case (i) With out-slip condition
Case (ii) With Slip condition

Fig. 1 Physical model of the problem with peristaltic effect.

The wall deformation is given by

$$Y = H(\bar{X}, \bar{t}) = a + b \sin \left[\frac{2\pi}{\lambda} (\bar{X} - c\bar{t}) \right], \quad (28)$$

Case (i) No-slip condition

The corresponding non-dimensional no-slip boundary conditions are

$$\frac{\partial u}{\partial y} = 0, \frac{\partial \Omega}{\partial y} = 0 \text{ at } y=0 \tag{29}$$

$$u = -1, \Omega = -1 \text{ at } y = h = 1 + \phi \text{Cos}(2\pi x)$$

Case (ii) Slip-condition

The corresponding non-dimensional slip-boundary conditions are

$$\frac{\partial u}{\partial y} = 0, \frac{\partial \Omega}{\partial y} = 0 \text{ at } y = 0 \tag{30}$$

$$u = -1 - \beta_1 \frac{\partial u}{\partial y}, \Omega = -1 - \beta_1 \frac{\partial \Omega}{\partial y} \text{ at } y = h = 1 + \phi \text{Cos}(2\pi x) \tag{31}$$

where $\beta_1 = \frac{\sqrt{Da}}{\alpha_1}$ with

Case(iii).Flow with Ciliated effect with no slip boundary condition

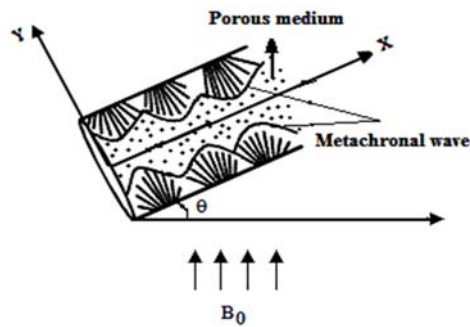


Fig. 2. Physical model of the problem with ciliated effect.

The inner surface of the channel is ciliated with metachronal waves and the flow occurs due to collective beating of the cilia.

The wall deformation is given by

$$\bar{Y} = a + a \varepsilon \text{Cos}\left[\frac{2\pi}{\lambda}(\bar{X} - c\bar{t})\right] \tag{32}$$

The cilia tips horizontal position may be expressed as

$$\bar{X} = \bar{X}_o + a\alpha \varepsilon \text{Sin}\left[\frac{2\pi}{\lambda}(\bar{X} - c\bar{t})\right] \tag{33}$$

and if no slip condition is applied, then the velocities of the transporting fluid are just those caused by the cilia tips, which can be given as:

$$\bar{U} = \frac{-\frac{2\pi}{\lambda} a \varepsilon \alpha \text{Cos}\left[\frac{2\pi}{\lambda}(\bar{X} - c\bar{t})\right]}{1 - \frac{2\pi}{\lambda} a \alpha \varepsilon \text{Cos}\left[\frac{2\pi}{\lambda}(\bar{X} - c\bar{t})\right]}$$

$$\bar{V} = \frac{-\frac{2\pi}{\lambda} a \alpha c \text{Sin}\left[\frac{2\pi}{\lambda}(\bar{X} - c\bar{t})\right]}{1 - \frac{2\pi}{\lambda} a \alpha c \text{Cos}\left[\frac{2\pi}{\lambda}(\bar{X} - c\bar{t})\right]}$$

The non-dimensional no-slip boundary conditions are

$$\begin{aligned} \frac{\partial u}{\partial y} = 0, \frac{\partial \Omega}{\partial y} = 0 \text{ at } y = 0 \\ u = -1 - \frac{2\pi\beta\alpha\varepsilon\text{Cos}(2\pi x)}{1 - 2\pi\beta\alpha\varepsilon\text{Cos}(2\pi x)}, \\ \Omega = -1 \\ \text{at } y = h(x) = 1 + \varepsilon \text{cos}(2\pi x) \end{aligned} \tag{34}$$

3. SOLUTION OF THE PROBLEM

Equations (26) and (27) together with the corresponding boundary conditions are solved to get the fluid velocity u , Micro-rotation vector Ω , pressure rise Δp and time average flow rate \bar{Q} .

The axial velocity is given by

$$u = \frac{1}{(M^2 + \sigma^2)L_1} \left\{ \begin{aligned} & \left[C_1 L_4 \text{Sinh}(m_1 y) + C_2 (L_4 \text{Cosh}(m_1 y) - L_5 \text{Cosh}(m_2 y)) - L_5 C_3 m_2 \text{Cosh}(m_2 y) \right] \\ & - L_1 \left(\frac{dp}{dx} + G \text{Sin} \theta \right) \end{aligned} \right\} \tag{35}$$

$$\Omega = C_1 \text{Cosh}(m_1 y) + C_2 \text{Sinh}(m_2 y) + C_3 \text{Cosh}(m_1 y) + C_4 \text{Sinh}(m_2 y) \tag{36}$$

The volume flux q through each cross section in the wave frame is given by

$$q = \int_0^h u dy \tag{37}$$

The time averaged flow rate is

$$\bar{Q} = q + 1 \tag{38}$$

Eliminating dp/dx from Eq. (35) we get pressure gradient as

$$\frac{dp}{dx} = \frac{(\bar{Q} - 1)(M^2 + \sigma^2)(1 - N) - L_{22} - L_2}{(1 - N)(L_{21} - h)} \tag{39}$$

Integrating the Eq. (39) over one wave length, we get the pressure rise (drop) for peristalsis with no-slip condition over one cycle of the wave as

$$\Delta p = \int_0^1 \frac{dp}{dx} dx \tag{40}$$

Case (i) Solution for no-slip condition with peristalsis:

$$m_1 = \sqrt{\frac{m^2 + AL_1 + \sqrt{(AL_1)^2 - (8m^2 AL_1 / (2 - N))}}{2}}$$

$$m_2 = \sqrt{\frac{m^2 + AL_1 - \sqrt{(AL_1)^2 - (8m^2(AL_1)/(2-N))}}{2}}$$

Case (ii) Solution for slip condition with peristalsis:

$$m_1 = \sqrt{\frac{m^2 + M^2L_1 + \sqrt{(M^2L_1)^2 - 8m^2M^2L_1/(2-N)}}{2}}$$

$$m_2 = \sqrt{\frac{m^2 + M^2L_1 - \sqrt{(M^2L_1)^2 - (8m^2M^2L_1)/(2-N)}}{2}}$$

Case (iii) Solution for no-slip condition with cilia:

$$m_1 = \sqrt{\frac{m^2 + AL_1 + \sqrt{(AL_1)^2 - (8m^2AL_1)/(2-N)}}{2}}$$

$$m_2 = \sqrt{\frac{m^2 + AL_1 - \sqrt{(AL_1)^2 - (8m^2AL_1)/(2-N)}}{2}}$$

4. RESULTS AND DISCUSSIONS

The governing equations are solved together with the corresponding boundary conditions to get fluid velocity u , Micro-rotation vector Ω and pressure rise Δp for varying Micropolar parameter m , magnetic parameter M , coupling number N and porous parameter. The variation of velocity u along y for Micropolar parameters $m=2.5$ to 4.5 for $\sigma=0.5, \varphi=0.4, M=1.3, N=0.2, \theta=\pi/3, \bar{Q}=1.5, \beta=0.2, \varepsilon=0.4, \alpha=0.7, \beta=0.2$ are shown in Fig. 3. From Figs. 3(a),3(b) and 3(c) it is observed that as the Micropolar parameter m increases the velocity decreases in all the three cases. However in case of slip condition with peristalsis Fig. 3(b), velocity is higher than the other two cases due to the slip at the boundary.

The Profiles of velocity and Micro rotation vector for different values of magnetic parameter M are shown in Fig. 4. It is observed that as the magnetic parameter M increases the velocity of the fluid decreases due to an increase in magnetic flux B_0 leads to increased Lorentz force. This force acts along the direction of flow leading to a higher velocity. Also it is analyzed from Figs. 4(a) and 4(c) that ciliated effect at the boundary reduces the velocity compared to no-slip with peristaltic effect for higher values of magnetic parameter M . In case of slip condition the value of velocity is significantly higher compared to no-slip and cilia effect for fixed value of M which can be analyzed from Fig. 4(b).

The profiles of velocity for different values of Coupling number N are shown in Fig. 5. It is observed that as N increases the velocity decreases beyond $y = -0.5$ to $y = 0.5$ in all the three cases. Increase in coupling number indicates increase in vortex viscosity, which

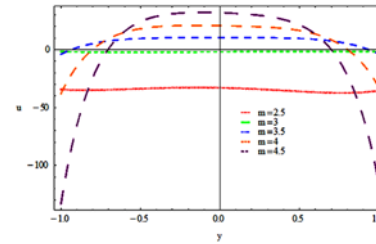


Fig. 3(a). Peristalsis with no-slip

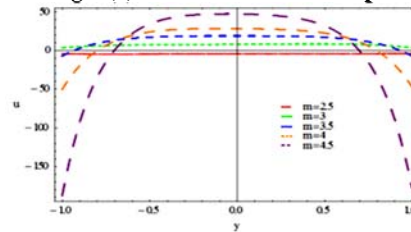


Fig. 3(b). Peristalsis with slip

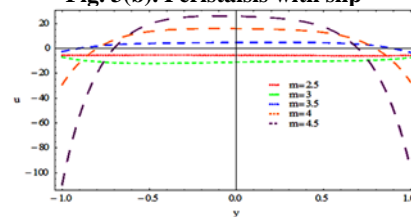


Fig. 3(c). With cilia

Fig. 3. Velocity profiles for different values of Micropolar parameter m (with peristalsis and cilia effects separately)

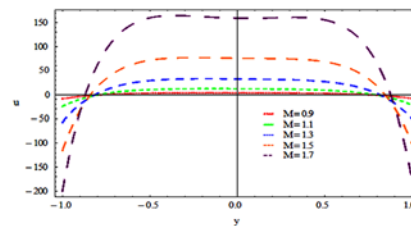


Fig. 4(a). Peristalsis with no-slip

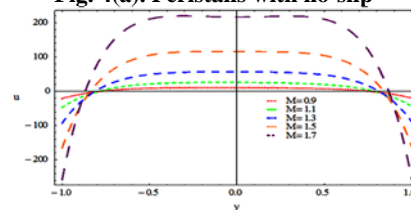


Fig. 4(b). Peristalsis with slip

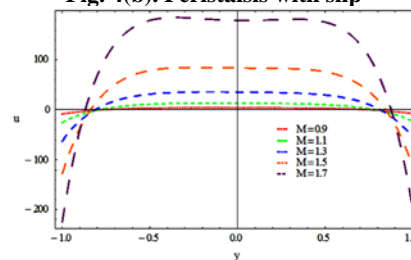


Fig. 4(c). With cilia

Fig. 4. Velocity profile for different values of magnetic parameter M (with peristalsis and cilia effects separately)

increases the momentum drag and hence reduces the velocity of the fluid which is depicted in the figures.

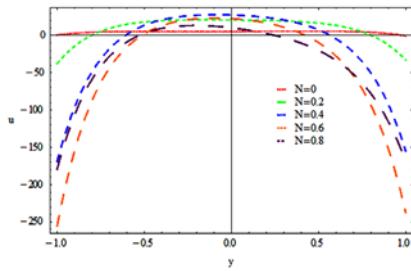


Fig. 5(a). Peristalsis with no-slip

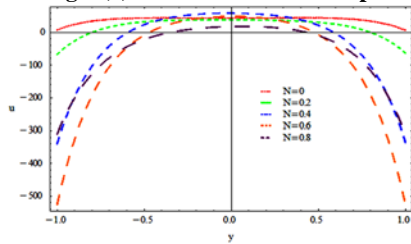


Fig. 5(b). Peristalsis with slip

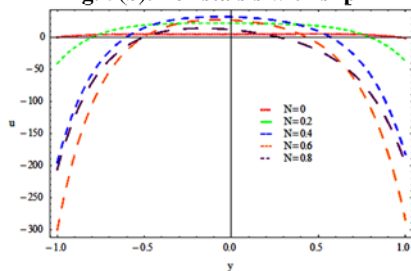


Fig. 5(c). With cilia

Fig. 5. Velocity profile for different values of coupling number N (with peristalsis and cilia effects separately)

The analysis is made on the effect of variation of porous medium on velocity when the fluid passes through the porous medium and past the porous medium. The porous parameter σ is given by $\sigma = a/\sqrt{k_0}$ where k_0 is the porous permeability and a the distance between origin and the boundary. It is observed from Fig. 6(a) that the presence of porous medium in the channel slows down the flow in case of no-slip condition with peristalsis compared to ciliated effect which is shown in Fig. 6(c). Also it is observed that the fluid velocity increases as the Darcy's number increases. Darcy's number is given by $Da = k_0/a^2$. Permeability is a measure of the ease with which a fluid can move through a porous medium. This implies that flow velocity would be higher for higher Darcy numbers a feature which is reflected in Fig. 6 (b).

The profiles of velocity for different values of angle of inclination are shown in Fig. 7. It is observed that velocity is insensitive to angle of inclination in all the three cases. This is due to the fluid's Reynolds number being very small leading to an inertia free flow.

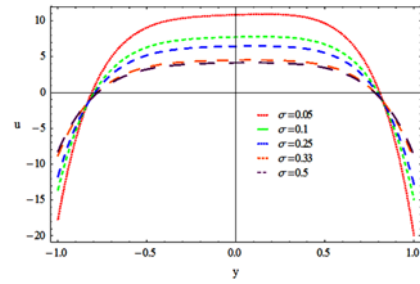


Fig. 6(a). Peristalsis with no slip

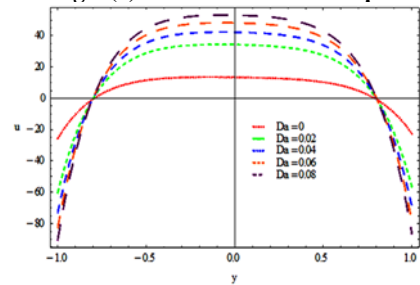


Fig. 6(b). Peristalsis with slip

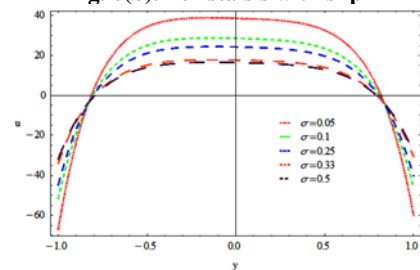


Fig. 6(c). With cilia

Fig. 6. Velocity profile for different values of porous parameter σ (with peristalsis and cilia effects separately)

The profiles of micro-rotation vector for different parameters are shown in the figures Figs. 8 – 11.

From Fig. 8, it is observed that as the Micropolar parameter $m = \sqrt{j^2 k(2\mu + k)}/\gamma(\mu + k)$ is a direct function of j , the gyration gradient and k , the vortex viscosity. Since both j and k represent rotational aspects, it is obvious that micro polar rotation is large for large values of Ω , since one rotational feature can couple better to another rotational feature.

It is interesting to note that for the increasing values of m the micro rotation vector Ω decreases at one end of the channel and shows reverse behavior at the other end for no-slip condition with peristaltic and ciliated effect which is shown in Figs. 8(a) and 8(c). Similar behavior is observed for slip condition with peristalsis which is shown in Fig. 8(b).

The effect of magnetic parameter M on rotation vector Ω is shown in Fig. 9. It is observed that for a Micropolar fluid as the magnetic parameter M increases Ω decreases for fixed value of y . From Figs. 9(a) and 9(c) it is observed that the effect of

variation of M on rotation vector Ω in the presence of peristalsis with no-slip condition and cilia is low compared to slip condition with peristalsis which is shown in Fig. 9(b).

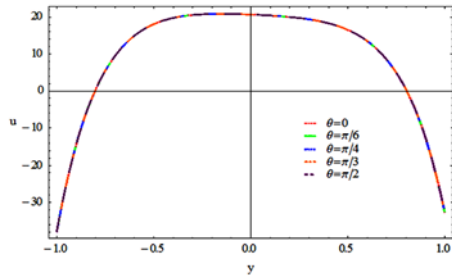


Fig. 7(a). Peristalsis with no-slip

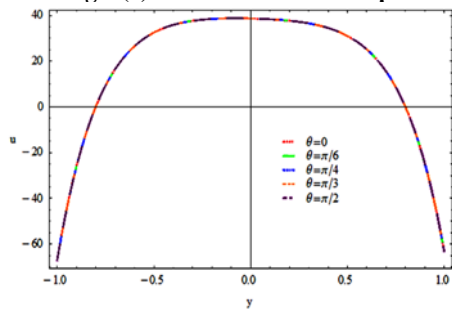


Fig. 7(b). Peristalsis with slip

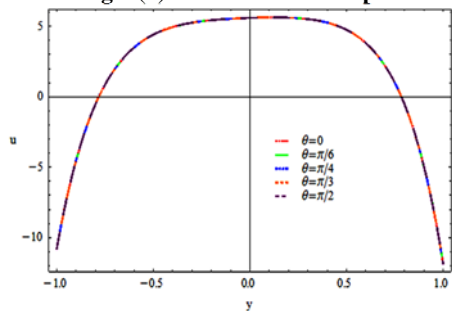


Fig. 7(c). With cilia

Fig. 7. Velocity profile for different values of angle of inclination (with peristalsis and cilia effects separately)

The effect of varying porous parameter on Microrotation profile is illustrated in Fig. 10. It is observed that for fixed value of y the magnitude of Micro rotation vector decreases as porous parameter increases. Also it is observed from Figs. 10(a) and 10(c) due to the presence of porous medium in the channel the magnitude of Microrotation vector is small compared to that due to the effect of slip condition which is shown in Fig. 10(b).

Pumping Performance

The pumping performance is characterized by means of the pressure rise per wavelength. The variation of time averaged flow rate \bar{Q} , with pressure rise per wavelength, Δp , for various parameters are given in Figs. 11 to 13.

The effect of Micropolar parameter m on

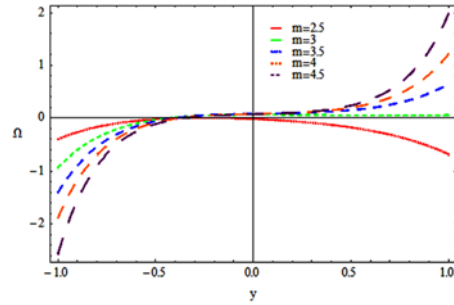


Fig. 8(a). Peristalsis with no-slip

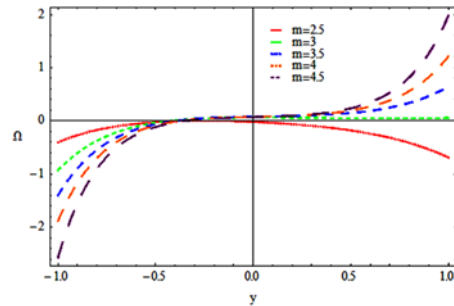


Fig. 8(b). Peristalsis with slip

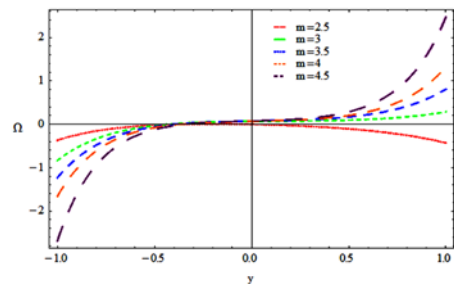


Fig. 8(c). With cilia

Fig. 8. Profile for micro rotation vector for different values of Micropolar parameter (with peristalsis and cilia effects separately)

pumping characteristics is shown in Fig. 11. It is observed that pressure rise Δp decreases as mean flow rate increases in the pumping region and reverse effect is observed in co-pumping region. The pumping due to peristalsis with no-slip condition is shown in Fig. 11(a), with slip condition is shown in Fig. 11(b) and pumping due to metachronal wave is depicted in Fig. 11(c). For fixed value of m the pressure rise is high with ciliated effect compared to peristaltic effect with no-slip, but when compared to slip-condition with peristalsis pressure rise higher than ciliated effect.

The variation of pressure rise with average flow rate \bar{Q} for different values of magnetic parameter M is shown in Fig. 12. It is observed that pressure rise Δp decreases as mean flow rate increases. For fixed value of \bar{Q} the pressure rise increases as magnetic parameter M increases in the pumping region and reverse effect is observed in co-pumping region. The pumping due to peristalsis with no-slip condition is shown in Fig. 12(a), with slip condition is shown in Fig. 12(b) and

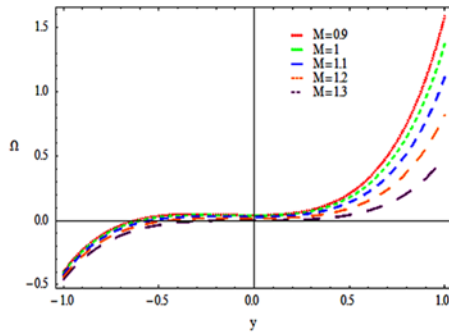


Fig. 9(a). Peristalsis with no-slip

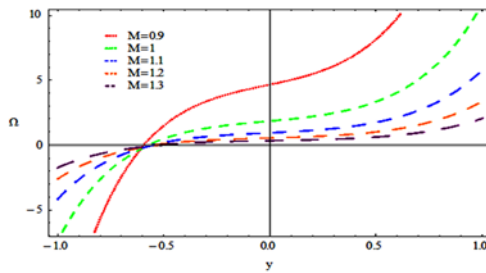


Fig. 9(b). With slip

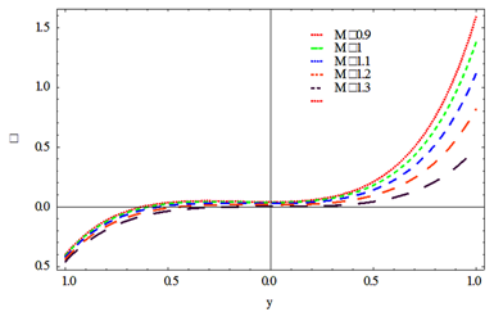


Fig. 9(c). With cilia

Fig. 9. Profile of Microrotation vector for different values of magnetic parameter M (with peristalsis and cilia effects separately)

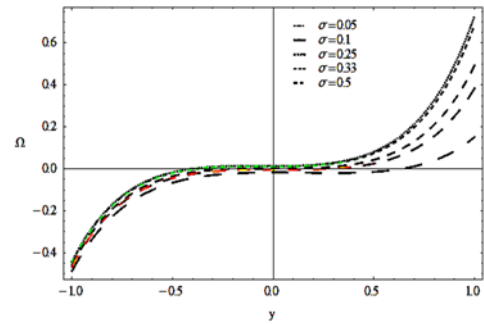


Fig. 10(a). Peristalsis with no-slip

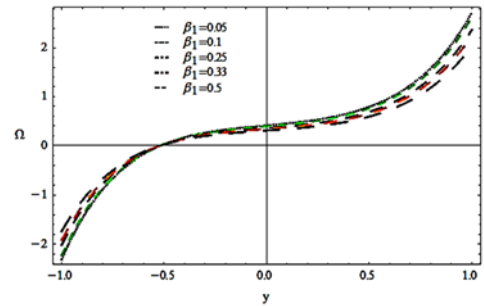


Fig. 10(b). Peristalsis with slip

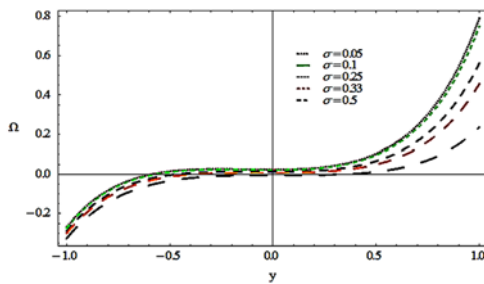


Fig. 10(c). With cilia

Fig. 10. Profile for Microrotation vector for different values of porous parameter (with peristalsis and cilia effects separately)

pumping due to metachronal wave is depicted in Fig. 12(c). For fixed value of M the pressure rise is high with ciliated effect compared to peristaltic effect with no-slip, but when compared to slip-condition with peristalsis pressure rise is higher than ciliated effect.

It is observed that as porous parameter increases the pressure rise increases in pumping region and reverse behavior is observed in co-pumping region in all the three cases which is shown in Fig. 13. From Fig. 13(c) it is observed that pressure rise is high due to metachronal wave of cilia.

5. CONCLUSIONS

An attempt is made to study the effect of peristalsis and cilia on the flow of MHD Micropolar fluid through a porous channel. Along with peristalsis, three cases are considered. i. slip boundary condition ii. no slip condition iii. Cilia.

Following are the conclusions drawn from the

study.

1) Increase in the micropolar parameter m increases the velocity in all the three cases. However in case of slip condition with peristalsis, velocity is higher than the other two cases due to the slip at the boundary.

2). Magnetic parameter M increases the velocity of the fluid decreases due to an increase in c leads to increase in Lorentz force. The ciliated effect at the boundary reduces the velocity compared to no-slip with peristaltic effect for higher values of magnetic parameter M . In case of slip condition the value of velocity is significantly higher compared to no-slip and cilia effect for fixed value of M .

3) Coupling number N increases the velocity decreases beyond $y = -0.5$ to $y = 0.5$ in all the three cases. Increase in coupling number indicates increase in vortex viscosity, which increases the momentum drag and hence reduces the velocity of the fluid which is shown in the graphs.

4). Presence of porous medium in the channel slows down the flow in case of no-slip condition with peristalsis compared to ciliated effect.

5). Velocity is insensitive to angle of inclination in all the three cases. This is due to the fluid's Reynolds number being very small leading to an inertia free flow.

6). For the increasing values of m the micro rotation vector Ω decreases at one end of the channel and shows reverse behavior at the other end for no-slip condition with peristaltic and ciliated effect. Similar behavior is observed for slip condition with peristalsis.

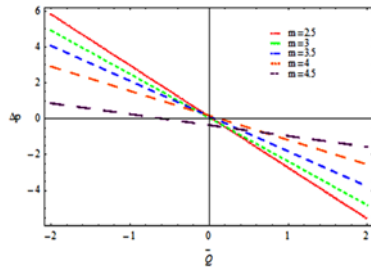


Fig. 11(a). Peristalsis with no-slip

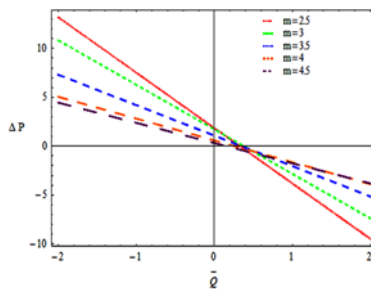


Fig. 11(b). Peristalsis with slip

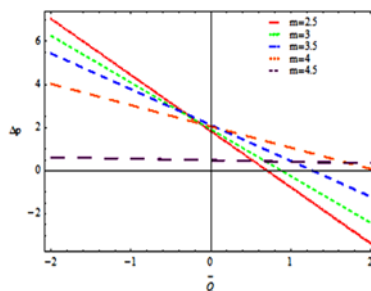


Fig. 11(c). With cilia

Fig. 11. Variation of pressure rise with average flow rate \bar{Q} for different values of Micropolar parameter m

7) The effect of varying porous parameter on Micro rotation profile is illustrated in Fig. 10. It is observed that for fixed value of y the magnitude of Micro rotation vector decreases as porous parameter increases. Also it is observed from Figs. 10(a) and 10(c) due to the presence of porous medium in the channel the magnitude of Micro rotation vector is small compared to that due to the effect of slip condition which is shown in Fig. 10(b).

8) The effect of Micro polar parameter, magnetic parameter and porous medium on pumping

characteristics also observed .

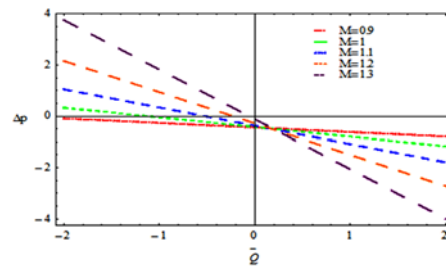


Fig. 12(a). Peristalsis with no-slip

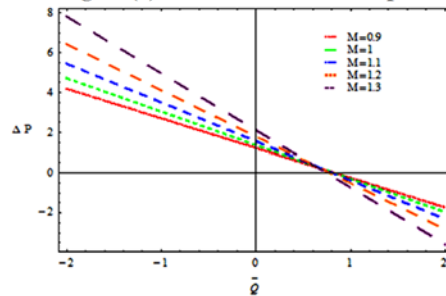


Fig. 12(b). Peristalsis with slip

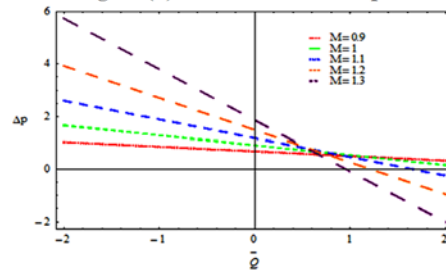


Fig. 12(c). With cilia

Fig. 12. Variation of pressure rise with average flow rate \bar{Q} for different values of magnetic parameter M

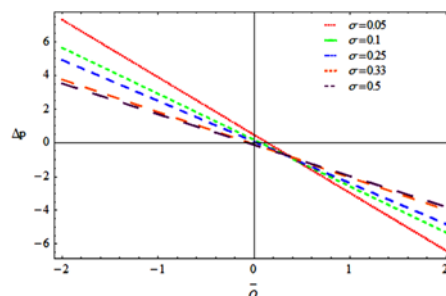


Fig. 13(a). Peristalsis with no-slip

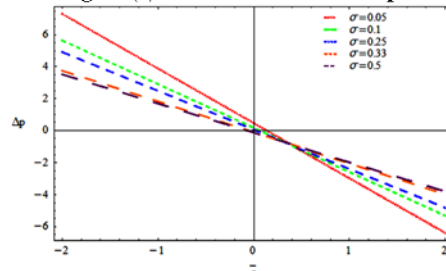


Fig. 13(b). With cilia

Fig. 13. Variation of pressure rise with average flow rate \bar{Q} for different values of porous parameter

REFERENCES

- Akbar, N. S., A. W. Butt, D. Tripathi and A. Bég (2017). Physical hydrodynamic propulsion model study on creeping viscous flow through a ciliated porous tube, *Indian Academy of Sciences*, 8852 – 61.
- Ariman, T. and A. S. Cakmak (1968), Some Basic viscous flows in Micropolar fluids, *Rheologica Acta*, Band 7, Heft 3, 236-242.
- Bear, J. (1972). *Dynamics of fluids in porous media*, American Elsevier Publishing Company, Inc., New York
- El Shehawey, E. F. and S. Z. A. Husseny (2000), Effects of porous boundaries on peristaltic transport through a porous medium, *Acta Mechanica*, 143, 165-177.
- El Shehawey, E. F., K. S. Mekheimer, S. F. Kaldas, and N. A. S. Afifi, (1999). Peristaltic transport through a porous medium, *J. Biomath.*, 14
- Eringen, A. C. (1965), *Theory of Micropolar fluid* ONR Report,
- Girija, Devi R. and R. Devanathan (1975), Peristaltic motion of a micropolar fluid, *Proc. Indian Acad. Sci.*, 81(A), 149-163.
- Gribben, R. J. (1965), The Magneto-Hydrodynamic boundary layer in the presence of a pressure gradient, *Proc. R. Soc. London*, 287, 123-141.
- Guirao, B. and J. J. Spontaneous (2017). Creation of Macroscopic Flow and Metachronal Waves in an Array of Cilia , Spontaneous Creation of Macroscopic , *Bio physical Journal*, 92, 1900-1917.
- Hayat, T., N. Ali, Q. Hussain, and S. Asghar (2008), Slip effects on the peristaltic transport of MHD fluid with variable viscosity, *Physics Letters A*, 372, 1477-1489.
- Krishna Kumari, P., S. V. H. N., Ravi Kumar, Y. V. K., M. V. Ramana Murthy and M. Chenna Krishna Reddy (2011), Peristaltic pumping of a Magneto hydrodynamic Casson Fluid in an Inclined channel, *Advances in Applied Science Research* 2(2), 428-436.
- Krishna Kumari. P, S. V. H. N. , Ravi Kumar Y. V. K., M. V. Ramana Murthy, Sreenadh (2011), Peristaltic pumping of Jeffrey fluid under the effect of a Magnetic field in an inclined channel, *Journal of Applied Mathematical Sciences* 5(9) , 447-458
- Mekheimer, K. S. (2003), Nonlinear peristaltic transport through a porous medium in an inclined planar channel, *J. Porous Media*, 6190-202.
- Moreau, R. (1990), *Kluwer Academic Publishers, Dordrecht*, The Netherlands.
- Muthu, B.V. Ratniskumar and P. Chandra, (2003), On the influence of wall properties in the peristaltic motion of Micropolar fluid. *ANZIAM J.*, 45 245-260.
- Satyanarayana, K., V. V., S. Sreenadh, P. Lakshminarayana and G. Sucharitha (2016), MHD peristaltic transport of a Micropolar fluid in an asymmetric channel with porous medium, *Advances in Applied Science Research*, 7, 105-114.
- Shaheen, A. and S. Nadeem (2017). Metachronal wave analysis for non-Newtonian fluid inside symmetrical. channel with ciliated walls, *Results in Physics*, 7, 1536 – 1549.
- Siddiqui, M., A. A. Farooq and M. A. Rana, (2015), A mathematical model for the flow of a Casson fluid due to metachronal beating of cilia in a tube, *The Scientific World Journal*, Article ID 487819, 12 pages.
- Srinivasacharya, D., M. Mishra and A. Ramachandra Rao, (2003), Peristaltic pumping of a Micro polar fluid in a tube, *Acta Mechanica*, 161, 165-178.
- Subba Reddy, M. V. and D. Prasanth Reddy, (2010), Peristaltic pumping of a Jeffrey fluid with variable viscosity through a porous medium in a planar channel, *International Journal of Mathematical Archive*, 1(2), 42-54.